

T-Jump/Time-of-Flight Mass Spectrometry for Time Resolved Analysis of Fast Condensed Stated Reactions

Lei Zhou, Nicholas Piekiet, Snehaunshu Chowdhury and Michael R. Zachariah*
*Department of Mechanical Engineering and Department of Chemistry and Biochemistry
University of Maryland, College Park, 20742, USA*

We describe a new T-jump/time-of-flight mass spectrometer for time-resolved analysis of rapid pyrolysis chemistry of solids and liquids, with a focus on energetic materials. The instrument employs a thin wire substrate which can be coated with the material of interest, and can be rapidly heated ($\sim 10^6$ K/s). The T-Jump probe is inserted with the extraction region of a linear-TOF mass spectrometer, which enables multiple spectra to be obtained during a single reaction event. By monitoring the electrical characteristics of the heated wire, the temperature can also be obtained and correlated to the mass-spectra. As an example, we present time-resolved spectra for the ignition of RDX and nanocomposite thermites. The fidelity of the instrument is demonstrated in the spectra presented which show the temporal formation and decay of several species in both systems. A simultaneous measurement of temperature enables us to extract the ignition temperature and the characteristic reaction time. The obtained time resolved mass spectra show that these solid energetic material reactions, under a rapid heating rate, can occur on a time scale of milliseconds or less. The capability of high speed time resolved measurements offers an additional analytical tool for characterization of the decomposition, ignition, and combustion of energetic materials

**Corresponding author. Email:mrz@umd.edu. Phone: 301-405-4311. Fax: 301-314-9477*

I. INTRODUCTION

Here we report on a new Time-of-Flight mass spectrometer (TOFMS) electron ionization (EI) source that can obtain time resolved mass-spectra during the ignition of energetic materials. The unique feature of this apparatus is a) implementation of TOFMS/EI with a Temperature Jump (T-Jump) technique to monitor highly reactive condensed state-samples at high heating and decomposition rates, and 2) measurement of the chemistry in a bi-molecular gas-phase-free kinetic environment. Due to its low detection limits and fast time response, the instrument developed here allows for a time resolved characterization of the decomposition, ignition, and combustion of solid energetic materials

Quantitative measurement of the condensed phase reaction kinetics are usually performed using conventional thermal analysis techniques[1] such as TGA (Thermogravimetric Analysis) and DSC (Differential Scanning Calorimetry). However, those methods fail in the measurement of fast chemistry processes such as rapid thermal decomposition, ignition and combustion of energetic materials where high heating rates are involved. It is well established that the high heating rates in those processes are critical and must be attained in order to study rapid condensed phase reactions.[2-4] In recent years, many experimental diagnostic methods have been developed to characterize rapid reaction processes.[1, 5-12] In particular, T-Jump (Temperature-Jump)/FTIR (Fourier Transform Infrared Spectroscopy) was developed for studying reaction kinetics of condensed-phase propellants.[2, 13] In the T-Jump/FTIR the sample is placed on a Pt filament and rapidly heated to a chosen temperature and the gaseous species are detected and quantified using FTIR spectroscopy. The thermal decomposition behavior of numerous energetic materials under isothermal conditions have been studied using this technique.[14-16] However, for rapid condensed phase reactions especially those associated with an ignition event, the relevant time scale can be on the order of milliseconds or less. The nominally low IR spectra scanning rate greatly limits the application of the T-Jump/FTIR spectroscopy in characterizing ignition, and combustion.

Mass Spectrometry (MS) is widely used to study condensed phase reactions.[12, 17] For decades, the use of MS alone or in conjunction with other techniques has become a powerful tool for thermal analysis.[10, 18-23] Blais and co-workers developed a TOFMS/EI apparatus capable of measuring the intermediates and products of chemical reactions from detonation of explosives.[10, 24] The decomposition of thermite based aluminum/iron (III) oxide energetic material was also studied using the Matrix-Assisted Laser Desorption/Ionization (MALDI)-TOFMS technique, and the products of laser initiated thermite reactions were identified.[25, 26] Time resolved measurements for condensed phase reactions have also been conducted using MS techniques. Dauerman and co-workers developed a scanning sector mass spectrometer which directly attaches to a low pressure strand burner to study the thermal decomposition and combustion of nitrocellulose.[11, 21] The sample is heated by exposure to the radiation of an arc image furnace and the gaseous species as well as the surface temperature are continuously analyzed by a mass spectrometer and thermocouple as a function of time. Behrens developed a thermogravimetric modulated beam mass spectrometer that combined thermogravimetric analysis, differential thermal analysis, and modulated beam mass spectroscopy. This instrument is capable of quantitative measurement, and has been used to study thermal decomposition mechanisms and kinetics of many compounds.[27-29] Korobeinichev and co-workers developed a pulse heated mass spectrometer to studied the high temperature decomposition of ammonium perchlorate.[30]

Common to all these methods has been that the studies were conducted at either slow heating rates, e.g. the thermal decomposition took place in minutes, or the mass spectrometer sampling rates were slow, e.g. ~ 0.1 sec. Recently, confined thermolysis FTIR spectroscopy with a TOFMS system has been used to analyze the gaseous products from a high pressure thermolysis chamber.[31] Although the time resolution of the mass spectra measurement can be ~ 1 ms, the system time response is limited by the slow sampling rate of the FTIR probe.

Despite the many efforts directed to characterizing condensed phase reactions, time resolved characterization of very rapid condensed phase reactions, particularly those associated with ignition and combustion have proved to be a formidable task. These processes, where the heating rates are usually of the order of $10^3\sim 10^6$ K/s, are beyond the limit of current thermal analysis techniques.[5, 32]

One additional consideration is that for many of the MS and FTIR studies, experiments were conducted in an open tube condition, such that much of the chemistry occurred in the gas-phase. However to gain a mechanistic understanding one would like to separate the condensed vs. gas phase contributions. Thus, in order to understand the decomposition mechanism or the combustion process of energetic materials, it is necessary to separate the primary and secondary processes, and investigate the condensed phase reaction under the condition of rapid heating.

Our objectives in developing the T-Jump-MS system was to be able to characterize chemistry under high heating rate conditions (i.e. fast chemistry), and to conduct the experiments under conditions where the secondary gas phase chemistry can be minimized. In the former case high heating rates correspond more closely to the environment usually encountered by energetic materials but more profoundly one should expect reaction channels to increasingly favor the higher activation channels possessing the lowest entropy constraints. The latter emphasis of minimizing gas-phase chemistry eliminates the possibility of bi-molecular gas phase reactions, leaving mostly unimolecular decomposition. As a result the rapid pyrolysis of energetic materials in vacuum should be dominated by condensed

phase reactions, which should ultimately allow for a more direct probe of condensed phase chemistry. The essence of the experiment is that the T-Jump probe is directly inserted into the Electron Ionization chamber of the mass spectrometer, and the species from T-Jump excitation are monitored by the TOF mass spectrometer continuously. The time-resolved mass spectrometric capabilities of the instrument enable the characterization of rapid solid state reactions, which should provide an insightful complement to conventional thermal analysis.

II. EXPERIMENTAL SECTION

A. EI/TOF Mass Spectrometer.

The EI/TOF mass spectrometer is comprised of a linear Time-of-Flight chamber, adapted from a previously developed Single Particle Mass Spectrometer (SPMS)[12, 33] and includes an electron gun for ionization, and the T-Jump probe with an electrical feedthrough, as shown in Fig. 1. The sample loading chamber is separated from the ionization chamber by a gate valve, which enables the T-Jump probe to be rapidly changed without the need to break vacuum in the TOF chamber. An electron gun is mounted between the extraction plates of the TOF, and perpendicular to the orientation of the T-jump probe. The electron beam is nominally operated at 70 eV, and 1 mA, with the background pressure in the TOF chamber at $\sim 10^{-7}$ Torr.

B. T-Jump Sample Probe and Sample Preparation.

In this work, nanocomposite thermites of Al/CuO and Al/Fe₂O₃ mixtures and Hexahydro-1,3,5-trinitro-1,3,5-triazine (RDX) were studied using the T-Jump/TOF mass spectrometer. For the T-Jump probe we have primarily used a 76 μ m diameter platinum wire, with a total heated length of ~ 1 cm, which is replaced after each heating event. Using an in-house built power source, the heating rate of the T-Jump probe can be varied by changing the pulse voltage or pulse width, at a rate of up to $\sim 8 \times 10^5$ K/s for the present filament configuration. The thermite mixtures or RDX were mixed with hexane or acetone, and a small amount of solution is coated on the T-Jump filament surface using a dropper. Nanocomposite thermite samples were prepared by mixing aluminum nanoparticles with an appropriate weight of oxidizer particles to obtain a stoichiometric mixture. The aluminum used was 50nm ALEX powder obtained from Argonide Corporation. Copper oxide (CuO) and iron oxide (Fe₂O₃) nanopowders of ~ 100 nm obtained from Sigma-Aldrich were used for mixing with the aluminum. TGA showed the ALEX powder to be 82% aluminum (by mass) with an oxide outer shell. This was considered in the preparation of stoichiometric samples (equivalence ratio of 1). Samples were mixed in hexane and the suspensions were sonicated for about 30 minutes to break the agglomerate and ensure intrinsic mixing between the fuel and oxidizer.

C. Control and Data Acquisition System.

The schematic of the control and data acquisition system for the T-Jump/TOF mass spectrometer is shown in Fig. 2. The present design is based on a previously developed Single Particle Mass Spectrometer (SPMS) which is configured for a standard laser ionization source.[12, 34] To ensure a field-free region for EI ionization, both the repeller plate and the extraction plate are grounded as shown in Fig. 2. In the presence of a field-free region, electrons are injected between the plates and ionization takes place. After a predetermined ionization period the voltage on the extraction plate is changed by a high voltage pulser, to create the field for an ion extraction region between the plates. The extracted ions drift in the linear TOF tube, and are counted at the MCP (Micro-channel Plate) detector. Following the ion extraction period, the voltage on the extraction plate is pulsed back,

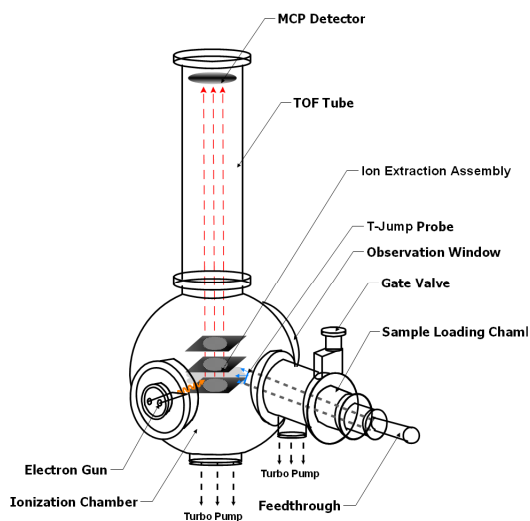


Figure 1. Schematic of T-Jump/TOF mass spectrometer.

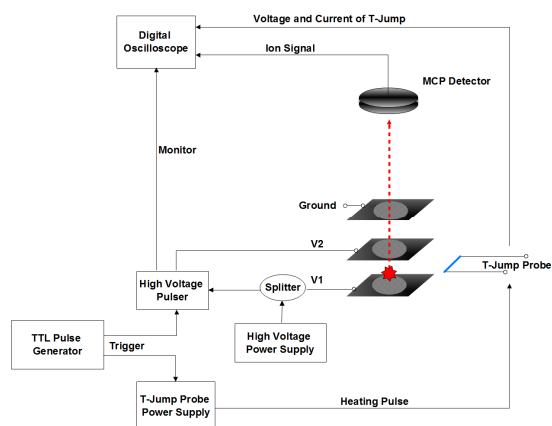


Figure 2. Schematic of the control and data acquisition system for the T-Jump/TOF mass spectrometer.

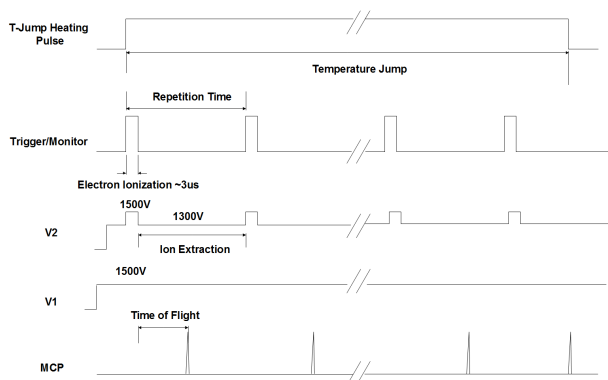


Figure 3. Pulse sequence used for EI and ion extraction in the T-jump/TOF mass spectrometer.

3 (There is $\sim 2 \mu\text{s}$ delay between the trigger and monitor signal, for illustration purposes we show them as the same pulse). The temporal voltage and current of the T-Jump probe during the heating event is recorded so that a resistivity measurement can be obtained, and related to the instantaneous temperature, which can be mapped against the mass spectra.

III. RESULT AND DISCUSSION

Before testing the T-Jump/TOF mass spectrometer, T-Jump probe heating experiments were conducted by heating an un-coated wire to evaluate the performance of T-Jump probe. The heating rate of the probe can be varied by changing the heating pulse width and the output pulse intensity. The pulse width can be varied from $\sim 1 \text{ ms}$ to $\sim 100 \text{ ms}$, with a maximum output voltage of $\sim 50 \text{ V}$. Figure 4 (a) shows a typical current and voltage trace, while Fig. 4 (b) shows the resulting temporal temperature of the platinum wire. Since the rise time of the heating pulse is in the range of 10 to $\sim 100 \text{ us}$ depending on the output pulse voltage, the resistance and the corresponding temperature is calculated after the rise time of the heating pulse. Thus the filament temperature is estimated to be $\sim 400 \text{ K}$ initially, and reaches $\sim 1800 \text{ K}$ after the 2.5 ms; i.e. a heating rate $\sim 640,000 \text{ K/s}$.

Al/CuO and Al/Fe₂O₃ nanocomposite mixtures were examined under rapid heating conditions. In each heating event, the T-jump probe was heated to $\sim 1700 \text{ K}$ with a $\sim 3 \text{ ms}$ voltage pulse, so that the heating rate is about $5 \times 10^5 \text{ K/s}$. Simultaneously, a sequence of 95 spectra with m/z up to 400 was recorded in a time resolved manner with a temporal resolution of 100 μs per spectrum. An example mass spectra for rapid heating of a Al/CuO sample were shown in Fig. 5 The first 41 mass spectra out of total 95 spectra are plotted, which corresponds to 0 to 4 ms of reaction time. The mass spectra in Fig. 5 clearly show the progression of the reaction as ion-species appear and then decay away. Similar results were obtained for other samples, but due to limitations of space, we select only one mass spectrum for each measurement, which provides an instantaneous snapshot of a reaction event for a particular stoichiometry or mixture and display the result Fig. 6. At the start of the heating event, $t = 0$, the spectrum recorded is that of the background in the ion source region, which consists of water ($m/z = 18$) as a primary species, and a small amount of N₂ ($m/z = 28$) and O₂ ($m/z = 32$) as shown in Fig. 6 (a). OH⁺ ions ($m/z = 17$) from e-impact fragmentation of water are also observed. As time advanced to the ignition point, the thermite reaction is initiated, and new peaks corresponding to reaction products can be observed. Figure 6 (b) is a typical mass spectrum for Al/CuO nanocomposite thermite reaction. New species of O ($m/z = 16$), Al ($m/z = 27$), CO₂ ($m/z = 44$), Cu ($m/z = 63, 65$) and Al₂O ($m/z = 70$) are identified. Similarly, Fig. 6 (c) is a mass spectrum obtained from an Al/Fe₂O₃ nanocomposite

and a new ionization period begins. Serial pulses generated from a pulse generator are used to trigger the high voltage pulser so that the ionization and extraction processes occur continuously. The pulse timing sequence of the high voltage pulse is also traced from the monitor signal output of the high voltage pulser. Both the detector signal and the monitor signal are recorded with a 500 MHz digital oscilloscope and transferred to a PC for further analysis.

The heating of the T-Jump probe is also synchronized with the time-of-flight measurement system by triggering the probe power supply from the pulse generator as shown in the timing sequence diagram in Fig.

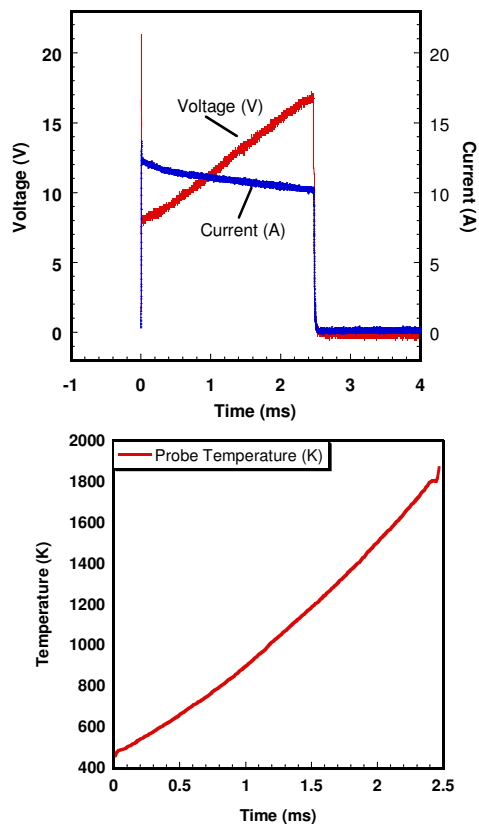


Figure 4 (a). Voltage and current across the T-Jump probe. (b). Estimated probe temperature from electrical resistance

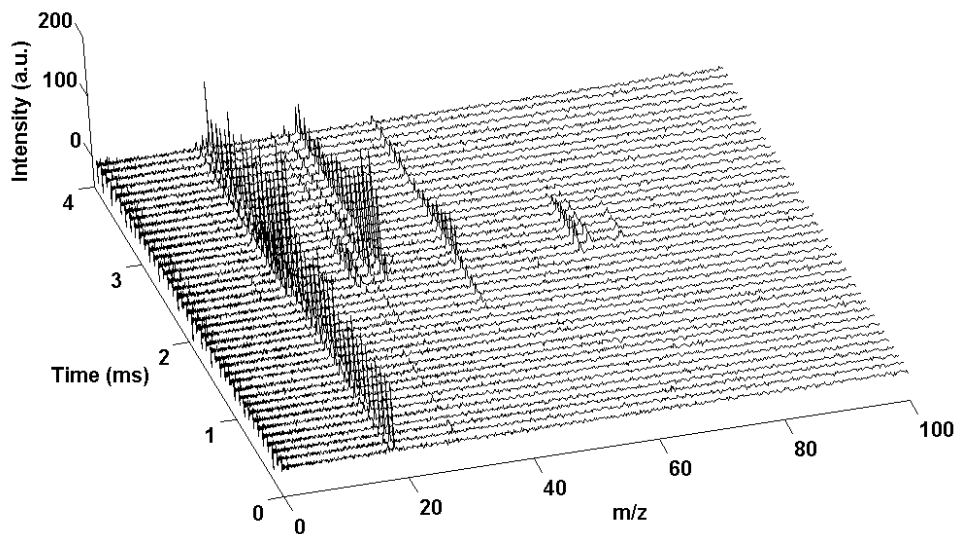


Figure 5 Time resolved mass spectrum from rapid heating of Al/CuO. Heating rate $\sim 5 \times 10^5$ K/s

experiment. New species of Al ($M/z = 27$), H_2CO ($m/z = 30$), CO_2 ($m/z = 44$), Fe ($m/z = 56$) and Al_2O ($m/z = 70$) are identified. No mass-spectral signals are observed that correspond to the hexane solution used to coat the particles, indicating that the sample is free of solvent effects.

One significant difference in Al/ Fe_2O_3 mass spectrum is the O ($M/z = 16$) and O_2 ($M/z = 32$) peak. Those peaks can be observed in Fig. 6 (c) but their intensities are much smaller than the Al/CuO case.

The mass spectra showed in Fig. 6 (b) and (c) enable us to identify the thermite reaction products. We first categorize these observed species into three groups. Species of Al, Al_2O , Cu, and Fe are the first category. Species of CO, H_2CO and CO_2 all contain carbon and are probably originated from the same source. Oxygen species O is presumed to be from fragmentation of the O_2 molecule during electron beam ionization, and form the third category. The species in the first category are compounds from nanocomposite thermite, and are apparently coming from thermite reaction. However the origin of the other species is ambiguous, by simply comparing with the background mass spectrum. Therefore, similar experiments were conducted for Al, CuO and Fe_2O_3 powders without mixing with their corresponding co-reactant and shown in Fig. 6 (d), (e) and (f), respectively. Al and Al_2O are observed in Fig. 6 (d) by simply heating Al powder. The Al_2O species is probably resulting from Al_2O_3 shell, while the Al peak suggests that the Al core will melt and leak out or diffuse out from the shell under heating. This has been previously observed by us in slow heating TEM imaging[35, 36]. Notice from Fig. 6 (e) and (f) that species of CO, H_2CO and CO_2 are only observed from heating of CuO and Fe_2O_3 particles. We also notice that the intensity of the water signal increases upon heating indicating that the powders have absorbed water. It is well known that water catalyzes the formation of copper carbonate ($CuCO_3$) shell on CuO particles or an iron carbonate ($FeCO_3$) shell on Fe_2O_3 particle. Upon heating the carbonate

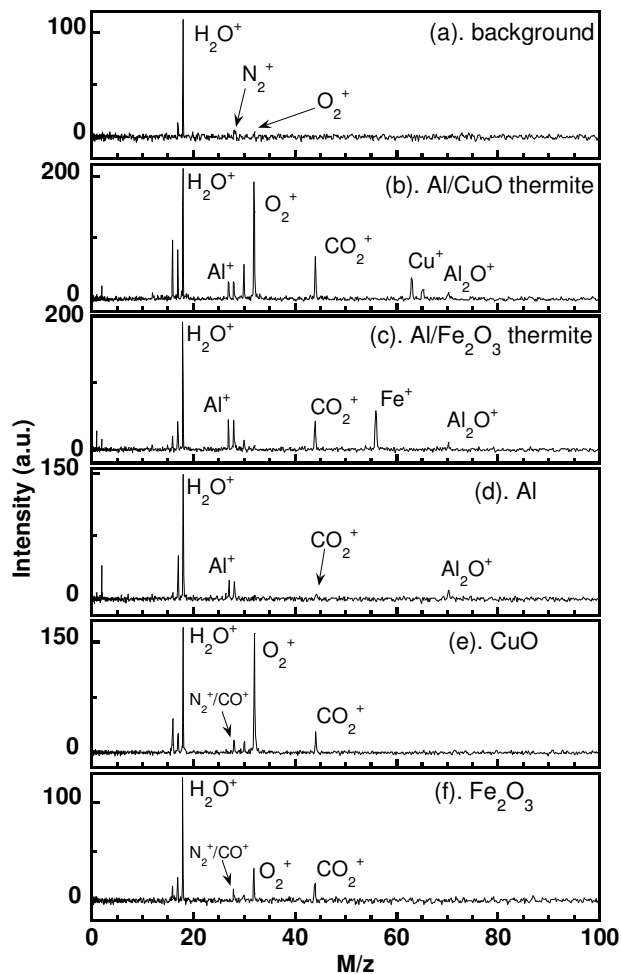


Figure 6 Selected mass spectra of nanocomposite experiments

shell decomposes to liberate, CO, H₂CO and CO₂ as identified in the spectra. Presumably this carbonate layer is only on the surface of particles, and should be very thin. The species in the third group (O, O₂) are of particular interest as free oxygen could be a key component in the reaction dynamics. As we can see in Fig. 6 (d), (e) and (f), no oxygen species are observed in heating of Al powder but a significant amount of O₂ is released from heating of CuO and Fe₂O₃ powder, implying that the oxygen observed during the thermite event are from the metal oxide particles. In addition, no Cu or Fe species is observed upon heating of CuO or Fe₂O₃ powder (Fig. 6 (e) and (f)), implies that the Cu or Fe peak observed in the thermite experiments should be a product from the thermite reaction.

As mentioned above, the mass spectra were recorded in a time-resolved manner. The normalized peak intensity of some major peaks as function of time are plotted and shown for an Al/CuO and Al/Fe₂O₃ in Fig. 7 (a,b) respectively. For both metal oxides we see that group 2 species CO (m/z = 28) and CO₂ (m/z = 44) appear before species from other groups, implying that the carbonate layer is first removed by thermal decomposition before the thermite event commences. As time advanced to ~ 1.8 ms in Fig. 7 (a) (Al/CuO mixture) or ~2.5 ms in Fig. 7 (b) (Al/Fe₂O₃ mixture), species of Al, Al₂O, Cu and O₂ (for Al/CuO) or Al, Al₂O and Fe (for Al/Fe₂O₃) begin to appear and ignition is considered to occur. The significant difference between Al/CuO system and Al/Fe₂O₃ system is the formation of oxygen species. The mass spectra of Al/CuO reaction show a strong O₂ peak, with a temporal profile (Fig. 7 (a)) following the same trend as other species, implying that oxygen is a reactive species, and involved in the thermite reaction. On the other hand, there is only a minor O₂ peak observed in mass spectra of the Al/Fe₂O₃ mixture reaction, despite the fact that oxygen release is observed in the heating of Fe₂O₃ particles. It is very likely then that O₂ formation from the metal oxide is important in the initiation of the thermite reaction. The oxygen specie is not only an oxidizer but may also behave as an energy propagation media that carries heat to neighboring particles,

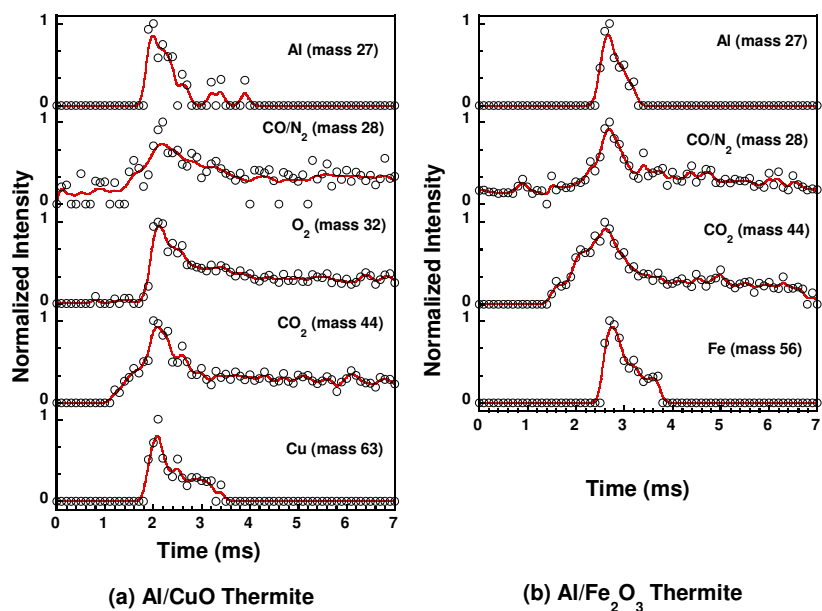


Figure 7 peak intensity as function of reaction time for nanocomposite thermite reactions

therefore, in contrast to the Al/CuO system where oxygen is generated in abundance, oxygen formation may become the limiting step for the Al/Fe₂O₃ reaction, and as a result, the Al/Fe₂O₃ reaction is much less aggressive compared to the Al/CuO system, despite the fact that their adiabatic temperatures do not differ significantly (Al/CuO 2837K VS Al/Fe₂O₃ 3135K). Based on these mass spectrometric observations, we can conclude that the reaction of the nanocomposite thermite system occurs in the following steps: (1) decomposition of CuCO₃ or FeCO₃ shell, (2) CuO or Fe₂O₃ decomposition ($4\text{CuO} \rightarrow 2\text{Cu}_2\text{O} + \text{O}_2$ or $6\text{Fe}_2\text{O}_3 \rightarrow 4\text{Fe}_3\text{O}_4 + \text{O}_2$), and melting and release of the Al core, (3) Al reacting with oxidizers. Here the metal oxide particles behave as an oxygen storage device, and can release oxygen very fast to initiate the reaction. This may also explain while aluminum particles burn much faster if mixed with metal oxide, than combustion in air.

To further understand the experimental mass spectrometric observation, thermal equilibrium calculations were conducted for Al/CuO and Al/Fe₂O₃ system using NASA CEA code. The system pressures were varied from room pressure to 10⁻¹¹ atm, and the calculated mole fraction of the resulting species were compared with the relative peak intensity measured from mass spectra. However, no good agreement can be found between the experimental results and the calculated mole fraction of reaction products. The thermal equilibrium calculation results show that Cu or Fe are dominant gaseous species, and the mole fraction of Cu or Fe are several orders of magnitude higher than gaseous Al or Al₂O. IN contrast the mass-spectra result shows that the oxide metal and that of Al are comparable. Another

species predicted by the equilibrium calculation is AlO, the mole fraction of gaseous AlO is slightly higher than that of Al₂O, however we only observed Al₂O, except under rich conditions (not discussed in this paper). These results imply that the combustion in the T-Jump experiments results in a highly non-equilibrium distribution of species.

RDX was used as a second example to test the T-Jump/TOF mass spectrometer. RDX decomposition has been the subject of many investigations under different conditions. Behrens and co-workers have studied RDX decomposition using the simultaneous thermogravimetric modulated beam mass spectrometry (STMBMS).[27, 37, 38] The results via STMBMS provide detailed information about both mechanisms and rates of reaction of RDX decomposition under a low heating rate (~1K/min). The combustion like decomposition of RDX has been studied using a T-jump/FTIR method[2-4, 13, 14, 39] with a heating rate at ~10³K/s. In our experiments, a heating rate of ~10⁵ K/s was used to study the ignition and combustion of RDX. Similar to the nanocomposite experiments, we use a sampling rate of 100 μs per spectrum (10,000Hz) to capture the progression of the reaction. The heating pulse is about 8 ms at a heating rate of ~1.5×10⁵ K/s, and a total of 95 spectra are obtained. Fig. 8 shows that species, other than background species (water/N₂/O₂), only appear from 0.7 ms - 2.6 ms, which corresponds to a wire temperature of 370K to 670K. Although a m/z range up to 400 was recorded for each spectrum, no heavy ions were observed above m/z 150. The major ions from RDX decomposition observed are m/z 15, 28, 29, 30, 42, 46, 56, 75 and 127. Small ions of m/z 14, 16, 41, 43, 81, 120 are also found in some spectra. The RDX mass spectra in terms of m/z values observed and their most likely ion structures are tabulated in table 2. Similar to the T-jump/FTIR method[2-4, 13, 14, 39], species of NO₂, CH₂O, NO, CO, HNCO are also observed by our T-jump/TOF mass spectrometer. Using gas phase CO₂ laser photolysis of RDX, which provided extremely high heating rates, Zhao et al. observed

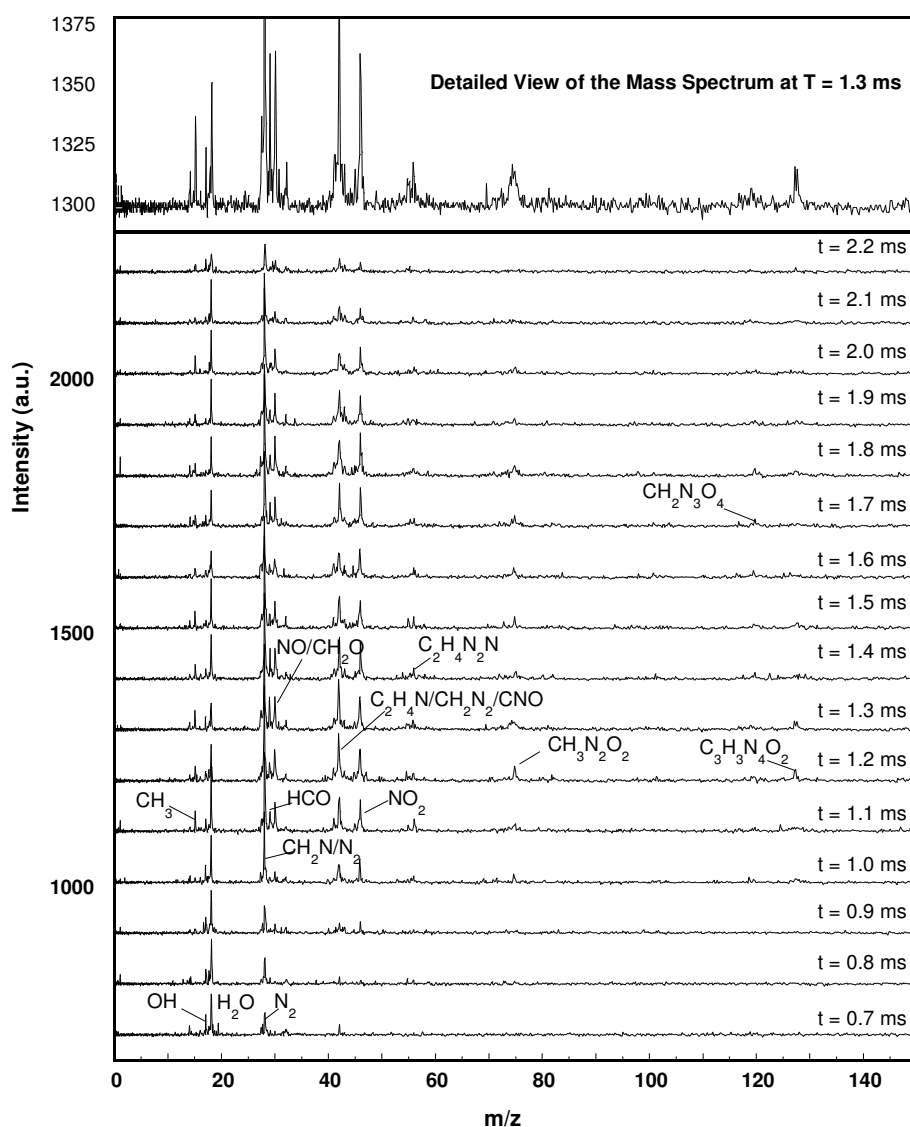


Figure 8. Time resolved mass spectrum from rapid heating of RDX. Heating rate ~1.5 ×10⁵ K/s

Table 1. ions observed from mass spectra of RDX pyrolysis and their possible assignments.

m/z	Species
14	N [#]
15*	CH ₃ , NH
16	O
17	OH [#]
18*	H ₂ O [#]
28*	N ₂ [#] , CH ₂ N, CO
29*	HCO
30*	NO, CH ₂ O
32	O ₂ [#]
41	CHN ₂
42*	C ₂ H ₄ N, CH ₂ N ₂ , CNO
43	HCNO
46*	NO ₂
56*	C ₂ H ₄ N ₂
75*	CH ₃ N ₂ O ₂
81	C ₃ H ₃ N ₃ (1,3,5-triazine)
120	CH ₂ N ₃ O ₄
127*	C ₃ H ₃ N ₄ O ₂

(*) major ions

([#]) species also observed in background MS

ions at 42, 56, 75, 81, 120 and 127, which we also see in our experiments[40]. However, HONO, HCN and N₂O which are reported in both T-jump/FTIR and gas-phase infrared multiphoton dissociation experiments were not detected under our conditions. The differences point to the complex nature that heating rate and ambient environment may play in probing the decomposition pathways. For example, it is believed that two global reactions are responsible for the decomposition of RDX under flash heating conditions.[13, 39] The reaction channel which leads to the formation of N₂O is dominant at the lower temperature regime, while the reaction channel to NO₂ favors a higher temperature condition. Our heating rate is much higher than the heating rate employed in T-jump/FTIR experiments (~10⁵ K/s vs. ~10³K/s) it is possible that the chemistry is dominated by the NO₂ channel and N₂O is not favored under these conditions. Moreover, as one of the motivations in developing this T-jump mass spectrometer, was to minimize or eliminate the gas phase chemistry, the failure to detect species such as HCN and HONO and possibly N₂O suggests these may be formed primarily in the gas phase.

Since the purpose of this paper is to demonstrate of the operation and capabilities of the instrument, we defer further analysis on rates of reactions and mechanisms to the future. Based on the experimental results presented above, it is clear that the characteristic reaction time for energetic material decomposition/combustion is on the order of milliseconds or even less. The experimental results suggest that the time-resolved spectra obtained using the T-jump/TOF mass spectrometer should have sufficient sensitivity, and time resolution to probe the reaction dynamics of extremely fast condensed state reactions at high heating rates.

IV. CONCLUSION

A new Time-of-Flight mass spectrometer (TOFMS) combined with a temperature jump technique is described. The instrument allows for the time resolved characterization of the decomposition, ignition, and combustion of solid energetic materials or other highly reactive condensed state reactions. Using heating rates of up to 10⁶ K/sec, samples of nitrocellulose and RDX were ignited, and time resolved mass spectra were obtained. By monitoring the electrical characteristics of the heated wire, the temperature could also be obtained and correlated to the mass-spectra. When combined with the time dependent temperature information, the results indicate that the instrument can capture the signature of rapid condensed phase reactions in a time resolved manner.

ACKNOWLEDGMENT

We thank Jack Touart in designing the T-Jump probe power supply. We also thank Dr. Jeff Hudgens of NIST for valuable advise during the course of debugging the instrument. We also gratefully acknowledge the funding support from the Army Research Office and the Defense Threat Reduction Agency.

REFERENCES

1. Vyazovkin, S., Thermal analysis. *Analytical Chemistry*, 2006. 78(12): p. 3875-3886.
2. Brill, T.B., et al., Surface Chemistry of Burning Explosives and Propellants. *J. Phys. Chem.*, 1995. 99(5): p. 1384-1392.
3. Brill, T.B., et al., T-Jump/FT-IR Spectroscopy: A New Entry into the Rapid, Isothermal Pyrolysis Chemistry of Solids and Liquids. *Applied Spectroscopy*, 1992. 46: p. 900-911.
4. Thynell, S.T., P.E. Gongwer, and T.B. Brill, Condensed-phase kinetics of cyclotrimethylenetrinitramine by modeling the T-jump/infrared spectroscopy experiment. *Journal of Propulsion and Power*, 1996. 12(5): p. 933-939.
5. Ward, T.S., et al., Experimental methodology and heat transfer model for identification of ignition kinetics of powdered fuels. *International Journal of Heat and Mass Transfer*, 2006. 49(25-26): p. 4943-4954.
6. Trunov, M.A., M. Schoenitz, and E.L. Dreizin, Ignition of aluminum powders under different experimental conditions. *Propellants Explosives Pyrotechnics*, 2005. 30(1): p. 36-43.
7. Furutani, H., et al., Laser-Induced Decomposition and Ablation Dynamics Studied by Nanosecond Interferometry. 2. A Reactive Nitrocellulose Film. *J. Phys. Chem. B*, 1998. 102(18): p. 3395-3401.
8. Makashir, P.S., R.R. Mahajan, and J.P. Agrawal, Studies on Kinetics and Mechanism of Initial Thermal-Decomposition of Nitrocellulose - Isothermal and Nonisothermal Techniques. *Journal of Thermal Analysis*, 1995. 45(3): p. 501-509.
9. Roberts, T.A., R.L. Burton, and H. Krier, Ignition and Combustion of Aluminum Magnesium Alloy Particles in O-2 at High-Pressures. *Combustion and Flame*, 1993. 92(1-2): p. 125-143.
10. Blais, N.C., H.A. Fry, and N.R. Greiner, Apparatus for the mass spectrometric analysis of detonation products quenched by adiabatic free expansion. *Review of Scientific Instruments*, 1993. 64(1): p. 174-183.
11. Dauerman, L., G.E. Salsler, and Y.A. Tajima, Characterization of Volatilized Species from Solid Propellants. *Aiaa Journal*, 1967. 5(8): p. 1501-&.
12. Mahadevan, R., et al., Measurement of Condensed-Phase Reaction Kinetics in the Aerosol Phase Using Single Particle Mass Spectrometry. *J. Phys. Chem. A*, 2002. 106(46): p. 11083-11092.
13. Kim, E.S., et al., Thermal decomposition studies of energetic materials using confined rapid thermolysis / FTIR spectroscopy. *Combustion and Flame*, 1997. 110(1-2): p. 239-255.
14. Hiyoshi, R.I. and T.B. Brill, Thermal decomposition of energetic materials 83. Comparison of the pyrolysis of energetic materials in air versus argon. *Propellants Explosives Pyrotechnics*, 2002. 27(1): p. 23-30.
15. Brill, T.B. and H. Ramanathan, Thermal decomposition of energetic materials 76: chemical pathways that control the burning rates of 5-aminotetrazole and its hydrohalide salts. *Combustion and Flame*, 2000. 122(1-2): p. 165-171.
16. Brill, T.B. and P.E. Gongwer, Thermal decomposition of energetic materials 69. Analysis of the kinetics of nitrocellulose at 50 degrees C-500 degrees C. *Propellants Explosives Pyrotechnics*, 1997. 22(1): p. 38-44.
17. Morelli, J.J., Thermal-Analysis Using Mass-Spectrometry - a Review. *Journal of Analytical and Applied Pyrolysis*, 1990. 18(1): p. 1-18.
18. Park, K., et al., Size-Resolved Kinetic Measurements of Aluminum Nanoparticle Oxidation with Single Particle Mass Spectrometry. *J. Phys. Chem. B*, 2005. 109(15): p. 7290-7299.
19. Mo Yang, J.M.R.B.J.K., Laser-induced Selective Dissociation of Nitro Groups in Nitrocellulose. *Rapid Communications in Mass Spectrometry*, 1996. 10(3): p. 311-315.
20. Jones, D.E.G., et al., The thermal decomposition of nitrocellulose. *International Annual Conference of ICT*, 2003. 34th: p. 46/1-46/17.
21. Dauerman, L. and Y.A. Tajima, Thermal Decomposition and Combustion of Nitrocellulose. *Aiaa Journal*, 1968. 6(8): p. 1468-&.
22. Farber, M. and R.D. Srivastava, A mass-spectrometric investigation of the chemistry of plateau burning propellants. *Combustion and Flame*, 1978. 31: p. 309-323.
23. Fowler, A.H.K. and H.S. Munro, A Preliminary Investigation of the Thermal and X-Ray-Induced Degradation of Cellulose Nitrates by Fab Sims and C-13 Nmr. *Polymer Degradation and Stability*, 1985. 13(1): p. 21-29.
24. Blais, N.C., R. Engelke, and S.A. Sheffield, Mass Spectroscopic Study of the Chemical Reaction Zone in Detonating Liquid Nitromethane. *J. Phys. Chem. A*, 1997. 101(44): p. 8285-8295.
25. Mileham, M.L., M.P. Kramer, and A.E. Stiegman, Laser Initiation Processes in Thermite Energetic Materials Using Laser Desorption Ionization Time-of-Flight Mass Spectrometry. *J. Phys. Chem. C*, 2007. 111(45): p. 16883-16888.
26. Stiegman, A.E., M.L. Mileham, and M.P. Kramer, Decomposition studies of thermite-based energetic materials using MALDI-TOF mass spectrometry. *Abstracts of Papers, 233rd ACS National Meeting, Chicago, IL, United States, March 25-29, 2007*, 2007: p. INOR-176.
27. Maharrey, S. and R. Behrens, Thermal Decomposition of Energetic Materials. 5. Reaction Processes of 1,3,5-Trinitrohexahydro-*s*-triazine below Its Melting Point. *J. Phys. Chem. A*, 2005. 109(49): p. 11236-11249.
28. Leanna Minier, Richard Behrens, and S. Bulusu, Mass spectra of 2,4-dinitroimidazole and its isotopomers using simultaneous thermogravimetric modulated beam mass spectrometry. *Journal of Mass Spectrometry*, 1996. 31(1): p. 25-30.
29. Behrens, R., New Simultaneous Thermogravimetry and Modulated Molecular-Beam Mass-Spectrometry Apparatus for Quantitative Thermal-Decomposition Studies. *Review of Scientific Instruments*, 1987. 58(3): p. 451-461.
30. Korobein, V.V. Boldyrev, and Y.Y. Karpenko, Use of a Pulse Mass Spectrometer to Investigate High-Speed Processes Associated with High-Temperature Decomposition of Ammonium Perchlorate. *Combustion Explosion and Shock Waves*, 1968. 4(1): p. 19-&.
31. Chowdhury, A. and S.T. Thynell, Confined rapid thermolysis/FTIR/ToF studies of imidazolium-based ionic liquids. *Thermochimica Acta*, 2006. 443(2): p. 159-172.
32. Umbrajkar, S.M., M. Schoenitz, and E.L. Dreizin, Exothermic reactions in Al-CuO nanocomposites. *Thermochimica Acta*, 2006. 451(1-2): p. 34-43.

33. Lee, D., K. Park, and M.R. Zachariah, Determination of the size distribution of polydisperse nanoparticles with single-particle mass spectrometry: The role of ion kinetic energy. *Aerosol Science and Technology*, 2005. 39(2): p. 162-169.
34. Wiley, W.C. and I.H. McLaren, Time-of-Flight Mass Spectrometer with Improved Resolution. *Review of Scientific Instruments*, 1955. 26(12): p. 1150-1157.
35. Rai, A., et al., Importance of Phase Change of Aluminum in Oxidation of Aluminum Nanoparticles. *J. Phys. Chem. B*, 2004. 108(39): p. 14793-14795.
36. Rai, A., et al., Understanding the mechanism of aluminium nanoparticle oxidation. *Combustion Theory and Modelling*, 2006. 10(5): p. 843 - 859.
37. Behrens, R. and S. Bulusu, Thermal decomposition of energetic materials. 4. Deuterium isotope effects and isotopic scrambling (H/D, ¹³C/¹⁸O, ¹⁴N/¹⁵N) in condensed-phase decomposition of 1,3,5-trinitrohexahydro-s-triazine (RDX). *J. Phys. Chem.*, 1992. 96(22): p. 8891-8897.
38. Behrens, R. and S. Bulusu, Thermal decomposition of energetic materials. 3. Temporal behaviors of the rates of formation of the gaseous pyrolysis products from condensed-phase decomposition of 1,3,5-trinitrohexahydro-s-triazine (RDX). *J. Phys. Chem.*, 1992. 96(22): p. 8877-8891.
39. Brill, T.B., et al., Condensed Phase Chemistry of Explosives and Propellants at High-Temperature - Hmx, Rdx and Bamo. *Philosophical Transactions of the Royal Society of London Series a-Mathematical Physical and Engineering Sciences*, 1992. 339(1654): p. 377-385.
40. Xinsheng, Z., J.H. Eric, and T.L. Yuan, Infrared multiphoton dissociation of RDX in a molecular beam. *The Journal of Chemical Physics*, 1988. 88(2): p. 801-810.